Article

Ultrasonic Non-Destructive Testing of Accelerated Carbonation Cured-Eco-Bricks

Joy Ayankop Oke [ID] and Hossam Abuel-Naga *

Civil Engineering Discipline, Department of Engineering, La Trobe University, Bundoora, VIC 3086, Australia; j.oke@latrobe.edu.au
* Correspondence: h.naga@latrobe.edu.au

Abstract: This study aimed to investigate the behavior of accelerated carbonation-cured laboratory specimens using the ultrasonic non-destructive testing (UNDT) method and compare the results with the destructive testing (DT) method. The materials used in the study included a blend of lime kiln dust and ground granulated blast furnace slag (LKD-GBFS) wastes, natural fine aggregate (sand), and alternative fine aggregates from waste tires. The chemical analysis of the LKD and GBFS samples highlighted them as suitable alternatives to OPC, hence their utilization in the study. A 60:40 (LKD-GBFS) blending ratio and a 1:2 mix design (one part LKD-GBFS blend and two part sand) was considered. The natural fine aggregate was partially replaced with fine waste tire rubber crumbs (TRCs) in stepped increments of 0, 5, and 10% by the volume of the sand. The samples produced were cured using three curing regimens: humid curing (HC), accelerated carbonation curing (ACC) with no water curing (NWC) afterwards, and water curing after carbonation (WC). From the results, an exponential model was developed, which showed a direct correlation between the UNDT and DT results. The developed model is a useful tool that can predict the CS of carbonated samples when cast samples are unavailable. Lastly, a total CO_2 uptake of 15,912 g (15.9 kg) was recorded, which underscores ACC as a promising curing technique that can be utilized in the construction industry. This technique will bring about savings in terms of the time required to produce masonry units while promoting a change in the basic assumptions of a safer and cleaner environment.

Keywords: accelerated carbonation curing; ultrasonic pulse velocity; compression strength; CO_2 uptake; scanning electron microscope; chemical analysis

1. Introduction

Research and reports have emphasized that the cement industry is predominantly responsible for emitting carbon dioxide gas (CO_2) and is a major energy consumer identified as a key driver of climate change [1,2]. Again, yearly reports show that the cement industry is responsible for about 5 to 8% of global anthropogenic CO_2 gas emissions [3,4]. Additionally, global emissions of CO_2 associated with producing cement reached about 2059 Mt in 2018. From this, emissions related to processing and energy accounted for about 66% and 34%, respectively [5]. The Global Status Report [6] further showed that in 2017, building and construction operations contributed about 36% of the global energy used and up to 40% of CO_2 emissions. This is because the construction industry has been adjudged as the highest global user of raw materials, and the built environment is responsible for about 25% to 40% of global greenhouse gas emissions [7]. This ranks ordinary Portland cement (OPC) as a major construction material whose sustainability is concerning [7–9] and has been receiving a lot of attention through various international initiatives and research [2,5–7,10–12].

The production of ordinary Portland cement, a major cementitious material globally used for construction, is responsible for significant environmental consequences [12,13]. These consequences include the discharge of highly concentrated energy due to a production temperature of about 1450 °C and a humongous amount of CO_2 emissions from other

industrial activities, contributing to about 5–8% of anthropogenic global warming [10,14]. By 2050, the demand for cement globally is projected to increase by 12–23% over the 2020 level, driven by spiraling urbanization, industrialization, and global population patterns, on top of infrastructure development needs [15]. To realign the cement sector with the Paris Agreement on global climate change, the annual emissions of CO_2 gas should drop by a minimum of 16% by 2030 [16]. The goal of the Paris Agreement is to mitigate global warming to below 2 °C, preferably to about 1.5 °C by the end of the current century [17,18], although records of global temperature show increments of 0.07 °C per decade from 1880 and over twice this increment since 1981 [19]. Hence, it is of utmost importance to lower the emissions linked to the manufacturing of cement. Furthermore, to plummet the global temperature increase, fast carbon dioxide sequestration (CO_2S) technologies involving the capture, utilization, and storage of (CUS) carbon are essential [20,21].

Due to this alarming rate of carbon emissions associated with OPC, research is constantly being carried out on the utilization of wastes (agricultural and industrial) as alternative cementitious material (ACMs) for developing cementless construction materials, units [22–27], and the utilization of captured CO_2 gas as a curing regimen [28–30] to enhance CUS. Additionally, quicker testing methods of these cementless construction units at the production stage are essential, emphasizing the importance of adequate quality control [26]. Quicker testing methods include the UNDT [26], ground-penetrating radar [31], and rebound hammer tests [32], which are all non-destructive.

In line with CUS, recent studies investigating the effect of CO_2S technologies on ACMs have been successfully performed [33,34]. Hwalla et al. [33] investigated the outcome of accelerated carbonation curing (ACC) on masonry units produced from alkali-activated slag. The study was carried out to assess masonry units' carbon sequestration performance, potentials, and microstructure. Factors such as the initial curing duration, carbonation pressure, and carbonation curing duration were varied for comparison purposes. The water absorption capacity and the compressive strength improved with higher pressure and extended initial curing and carbonation durations. Furthermore, going by the global warming potential index, the carbon footprint of the carbonated samples was up to 46%, which was lower when compared to the non-carbonated counterparts, as is necessary to mitigate CO_2 emission.

Muthu et al. [34] subjected a mix of electric arc furnace (EAF) slag and Wollastonite to CO_2 curing. It was reported that replacing cement with EAF slag at a higher volume resulted in volumetric expansion. To prevent this, the samples were carbonated with a CO_2 gas of high purity. This resulted in the development of non-expansive products that included aragonite, calcite, and remains of tobermorite within the matrix microstructure. The EAF slag was added to the Wollastonite at 0%, 20%, 40%, and 60% increments. The sample with 40% slag had the maximum compressive strength (CS), whereas the sample produced with 60% slag had the least CS. It was concluded from the study that utilizing EAF slag in the perspective of the investigation would advance CO_2 sequestration and avert the dumping of industrial waste into landfills.

In line with performing rapid NDTs, which are tests that do not set off structural damage or destruction to the units, the use of ultrasonic pulse velocity (UPV) is receiving attention. However, there is limited current research on its application in ACC units. UPV involves using longitudinal (P) or shear (S) waves to estimate the strength of these units. The P waves are preferred over the S waves due to their higher velocity, easy generation, and measurement [35,36].

In a study on the evaluation of rubbercrete samples, Mohammed et al. [35] considered the use of non-destructive tests (UPV and rebound hammer) and destructive tests (compression) to establish a relationship between the non-destructive and destructive test results. After the experiments, an exponential model was selected as the most preferred, which could be used to show a correlation between the non-destructive test (NDT) and the destructive test (DT). Furthermore, they concluded that between the UPV and rebound hammer tests, the UPV utilizing P waves was more reliable for evaluating rubberized samples.

In another study, Choi et al. [37] investigated the strength properties of rubberized concretes to show a correlation between the NDT and DT using P waves and compression tests, respectively. The exponential model was selected as the most preferred model with an acceptable trendline, which could be used to validate experimental data to relate the NDT to the DT. In their conclusion, the P wave was recommended for estimating the CS of rubberized concretes as a quicker testing option.

In summary, the highlighted challenges include the prominent levels of pollution caused by industrial activities, the production and use of OPC, and the disposal of wastes through landfills, which all imply a scaled-up emphasis on the need for sustainability in construction industries. From one perspective, ensuring that the products from the construction industry do not cause a high degree of carbonation is necessary. On the other hand, it is vital to ensure that the waste generated is reused in the construction industry while conserving energy [38–42]. It is also important to engage with technologies that will guarantee a reduction in the extraction of raw materials for construction purposes, such as utilizing alternative aggregates, so that these natural resources in the form of aggregates are not depleted [26,27,43,44]. Furthermore, it is essential to test units produced with wastes non-destructively as a quick test to ascertain their strength properties, utilizing the P wave as recommended by research [35–37]. Therefore, it is imperative to develop durable, green, readily available, and cost-effective construction materials that will address these highlighted issues without jeopardizing building quality or compromising on quality control.

This write-up on utilizing an LKD-GBFS blend as an ACM aims to substitute OPC fully, which involves finding an eco-gradient with the ACC treatment that produces bricks with a minimum of 3 MPa compressive strength. This act will promote LKD-GBFS as sustainable waste in construction while attempting to address the problems associated with the disposal of LKD in landfills. Furthermore, the continuous release of CO_2 into the atmosphere due to human activities discussed above underscores the need to investigate carbonation as a curing regimen. This will contribute to reducing the amount of CO_2 in the atmosphere and present itself as a quicker curing approach to save the time involved in producing masonry units, which usually takes 28 days. Additionally, this paper investigates the potential use of ultrasound methods to test the strength of cementless ACC-eco bricks produced with LKD-GBFS. This testing method has been established as a quicker testing method but has not been fully investigated on units produced with an LKD-GBFS blend and cured using ACC. Hence, this study has been conceived to fill this knowledge gap. Lastly, incorporating TRCs as an alternative aggregate to natural sand will aid in reducing the pressure exerted on it and prevent its gradual depletion.

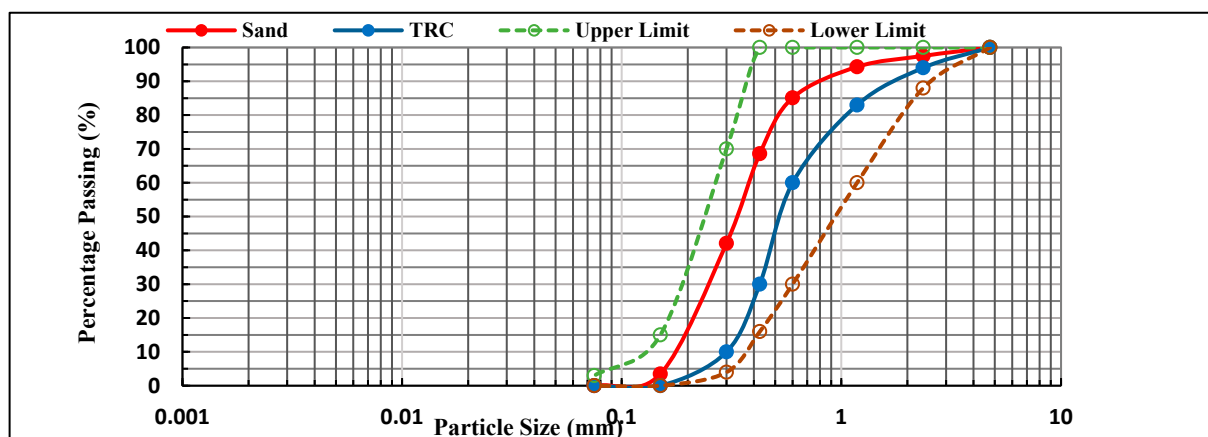## 2. Materials and Experimental Methods

2.1. Materials

LKD is the by-product of quick lime from high-temperature rotary kilns in powder form, which has a high calcium content but is mostly dumped in landfills [45]. Ground granulated blast furnace slag (GBFS), on the other hand, is an alternative cementitious material (ACM) that is composed of CaO, SiO_2, and Al_2O_3. Both samples (LKD and GBFS) were analyzed, and their oxides were compared to OPC samples from previous research. Table 1 shows the significant oxides in LKD, GBFS, and OPC samples. Furthermore, specific gravity (Gs) test values of 2.75 and 2.65 were obtained for the LKD and GBFS samples, respectively.

Table 1. Significant oxides in LKD, GBFS, and OPC samples.

Chemical Oxide (%)	LKD	GBFS	OPC [46]	OPC [47]
CaO	63.24	42.10	60.00–67.00	62.25
SiO_2	20.04	33.10	17.00–25.00	21.00
Al_2O_3	4.90	13.20	3.00–8.00	5.90
Fe_2O_3	3.49	0.30	0.50–60	3.40
MgO	1.11	6.50	0.01–40	1.50
K_2O	0.35	-	0.50–1.30	0.45
Na_2O	0.43	0.50	0.05–1.30	0.20
SO_3	2.35	2.00	1.00–3.00	2.40

From the oxide compositions obtained in Table 1, the presence of CaO, SiO_2, Al_2O_3, Fe_2O_3, and MgO with chemical oxide proportions of 63.42, 20.04, 4.90, 3.49%, and 1.11%, respectively, established LKD as a suitable replacement to OPC. However, an ACM having an elevated SiO_2 content with a minimum of 30% needs to be mixed with the LKD to further improve the cementitious property of the LKD [40,48]. Hence, GBFS with a SiO_2 of 33.1% was blended with the LKD. The elevated CaO and SiO_2 contents in the mix alongside the carbonation enhanced the strength of the samples.

Fine waste tire rubber crumbs (TRCs) obtained from waste tires were used to replace sand partially in stepped increments of 5 and 10% by the volume of sand. These waste tires were shredded to reduce their sizes and were fed into the granulator to liberate the steel from the rubber. After the liberation process, the wires were separated from the rubber through a magnetic separation process, then the crumbs were reduced to obtain the desired sizes of aggregates, between 0.06 and 10 mm, as recommended by He et al. [49]. Furthermore, the TRC was treated with sodium hydroxide (NaOH) 10% (*w/v*) for 24 h, as recommended by Tian et al. [50], Mohammadi et al. [51], and Guo et al. [52]. This was carried out to improve the hydrophilicity of the rubber, which made the rubber surface relatively rough and porous to aid bonding between the LKD-GBFS–sand matrix. Figure 1 shows the curves obtained from the particle size analysis of the sand and TRC. The fineness modulus (FM) and Gs of the sand and TRC were obtained to be 2.47, 2.96, 2.61, and 0.77, respectively.

Figure 1. Particle size analysis of TRC and fine sand.

2.2. Experimental Methods

In this study, a 1:2 design mix and a blending ratio of 60:40 (LKD: GBFS) were considered. One part by the weight of the LKD: GBFS blend to two parts by the weight of the natural aggregate (sand) as well as a water binder (w/b) ratio of 0.4 was used to produce the 0% TRC samples. Compression was carried out in 3 layers for each sample, and compression pressures of 1.2, 1.6, and 1.9 MPa were applied to each layer for 3 min. For the samples that contained TRC, the sand was replaced partially by the TRC in stepped

increments of 5 and 10% by the volume of the sand. The TRC improved the workability of the mix due to its low density. HC was performed for 72 h, ACC durations varied between 30, 48, and 72 h, and post-carbonation hydration was for 72 h. A minimum strength of 3 MPa for non-structural bricks was the target compressive strength in this research.

2.2.1. Sample Preparation

- Here, 234 samples were prepared per standards [53,54]; after that, the mix was transferred into greased formworks measuring 100 mm in height (H) and 50 mm in diameter (Ø) in three layers.
- The top of each layer was scarified before the next layer was introduced into the form. The scarifying was carried out so the new layer would act homogeneously with the previous layer. When the compression was completed, the samples were de-molded, and one set of samples was wrapped and allowed to cure in a humid environment (79 ± 5% and 19 ± 5 °C) for 72 h. The samples for carbonation were allowed to precondition for 4–6 h in a dry environment (RH = 55 ± 10%, T = 22 ± 3 °C) before carbonation [55–57].

2.2.2. Curing Method

The procedure for CO_2 curing is highlighted below:

- After pre-conditioning, the samples were labeled and introduced into the curing chamber as shown in Figure 2. A vacuum was applied into the chamber for 2–10 min at a pressure of about 600–1000 mm Hg [58,59].
- Immediately after vacuuming, CO_2 gas was released into the carbonation chamber for the curing duration considered in this study (30, 48, and 72 h). The purity of the CO_2 gas was at 99.9%, and the pressure was kept constant at 0.13–0.15 MPa (1.3–1.5 bar), which did not exceed 0.2 MPa (2 bar) [60,61].
- After the curing durations had elapsed, the samples were brought out of the curing chambers, weighed immediately, and divided into 2 sets. The first set was placed on the laboratory bench for 2 days before testing. The second set of samples was subjected to post-carbonation hydration (WC) in water tanks for 72 h immediately after weighing [61].

Figure 2. Carbonation set-up.

Post-carbonation hydration is necessary to restore the water lost during the precondition and carbonation stages. During carbonation, exothermic reactions occur, hence the post-carbonation hydration restores this water and promotes the secondary hydration of the unreacted hydraulic cement phases [61]. The exothermic reaction takes place between

the captured CO_2 gas and the calcium-bearing cementing materials in aqueous conditions and is represented by Equations (1) and (2) below [62,63].

$$3CaOSiO_2 + (3-x)CO_2 + yH_2O \rightarrow xCaOSiO_2yH_2O + (3-x)CaCO_3 \tag{1}$$

$$2CaOSiO_2 + (2-x)CO_2 + yH_2O \rightarrow xCaOSiO_2yH_2O + (2-x)CaCO_3 \tag{2}$$

After 72 h of post-carbonation curing, the samples were brought out of the water tanks and allowed to sit for 2 days; then, they were tested.

2.2.3. CO_2 Uptake

The mass-gain method was used to calculate the CO_2 uptake within the samples. This method focuses on determining the CO_2 uptake of the entire sample as an average, which gives an estimate of the CO_2 uptake by comparing the mass of the sample before and after carbonation. Due to carbonation being an exothermic reaction, the evaporation of water within the sample is hastened, and the evaporated water is collected and added to the final mass. Furthermore, the carbonation system is considered a closed system; hence, it is vital to consider the evaporated water because this water was originally part of the samples before the carbonation process [64]. From the study carried out by Xian et al. [65], El-Hassan and Shao [55], and Mahoutian and Shao [66], the equations that could be used to compute CO_2 uptake in samples are highlighted in Equations (3) and (4) below, which consider the mass-gain method.

$$CO_2 \text{ uptake } (\%) = \frac{Final\ mass + Mass\ of\ water\ loss - Initial\ mass}{Mass\ of\ dry\ cementing\ agent} \times 100\% \tag{3}$$

$$CO_2 \text{ uptake } (g) = \frac{CO_2\ (\%)}{100} \times Final\ mass\ after\ carbonation \tag{4}$$

3. Tests

3.1. Ultrasonic Non-Destructive Test (UNDT)

An ultrasonic pulse velocity (UPV) test is a form of UNDT that utilizes pressure (P) waves and shear (S) waves. These generated waves can be used to determine the strength of samples. Research has shown that mathematical models can be used to predict the strength of samples using P waves [26]. The advantages of using UPV include saving time and the fact that the test allows samples to be re-used for other purposes since the samples are not destroyed during testing. The UPV test was carried out using a Pundit PL-200 testing machine (Proceq, Schwerzenbach, Switzerland) to determine the passage of P waves through the samples. Vaseline was applied to the surface of the samples to maintain continuous contact between the sample and the transducers while testing. The transducers were placed on the samples as shown in Figure 3 below, and the transmitted waves were determined per standards [67].
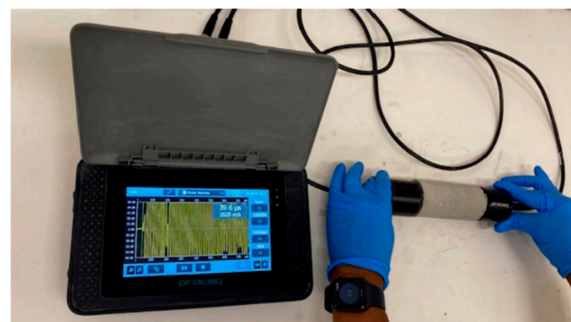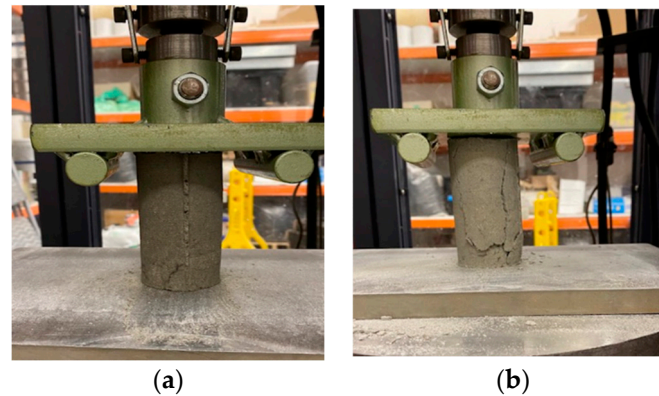

Figure 3. UNDT test in progress using UPV.

3.2. Destructive Test (DT)

A compression destructive test was conducted on the samples to determine the maximum force that would cause the sample's failure. This was achieved using the MTS compression testing machine with a capacity of 500 kN $\pm$ 25 kN. Figure 4a,b show the samples in the MTS machine before and after compression.

(a)   (b)

Figure 4. (**a**) Sample before compressing. (**b**) sample after compressing.

The compressive load on the samples was applied at a rate of 4 mm/min, and the procedure for the testing was carried out as per codes [53,54]. To obtain the compressive strength (*CS*), Equation (5) below was used:

$$CS = \frac{1000P}{A} \tag{5}$$

where

CS = Compression strength (N/mm^2);
P = The load that caused the failure (kN);
A = Area of the sample (mm^2).

3.3. Microanalysis

Scanning Electron Microscopy (SEM) and Energy Dispersive X-ray Spectroscopy (EDS) were carried out to analyze the carbonated and post-carbonation hydrated samples. The SEM and EDS were performed to ascertain the quantitative and qualitative composition of the elements in the samples, which gave a better understanding of the strengths achieved. The samples prepared with 0 and 5% were considered, and detailed high-resolution images were obtained, which are discussed in the results section.

The samples were mounted on aluminum stubs using a combination of carbon tape and conductive silver adhesive. The samples were imaged uncoated with a Hitachi SU7000 (Hitachi High-Tech Corporation, Tokyo, Japan) field emission SEM at an accelerating voltage of 15 kV, using the backscatter detector. The elemental compositions of the selected sites were collected with an Oxford EDS and were represented as plots with the energy in kiloelectronvolt (keV) on the abscissa and the intensity in counting photons per electron volt (cps/eV) on the ordinate.

4. Discussion of Results

A total of 234 samples were prepared with varying TRC contents. The different compression pressures of 1.2, 1.6, and 1.9 MPa, the three different curing approaches (HC, NWC, and WC), and the curing durations were analyzed. The samples were first tested non-destructively with the UPV machine and then tested destructively using the compression testing machine.

4.1. UNDT (Ultrasonic Pulse Velocity Test) and DT (Compression Test)

4.1.1. UNDT (Ultrasonic Pulse Velocity Test)

Figure 5 below shows a comparison of the P-wave velocities at different compression pressures and curing durations for the 0% TRC samples. In this result, three sets of samples were considered. The first were the samples that were wrapped and cured in a humid environment (HC), the second were the samples that were tested after the carbonation durations with no water curing afterward (NWC), and the third were the samples that were hydrated for 72 h in water (WC) after carbonation. All the samples cured with CO_2 gas (NWC and WC) had improved strength compared to the HC samples. This highlights carbonation as a preferred curing approach. Additionally, analyzing the ACC samples (NWC and WC) shows that the WC samples had improved strengths compared to the NWC samples. This shows that post-carbonation hydration is essential to restore the water lost in the samples during pre-conditioning and carbonation, thereby enhancing the secondary hydration of unreacted hydraulic cementitious pastes [61]. Furthermore, the samples with maximum velocities were those compressed with 1.9 MPa. This again shows that to obtain the optimum strength for carbonated samples, the samples should be compressed with a steady pressure of no less than 1.9 MPa, as recommended by research [60,68].
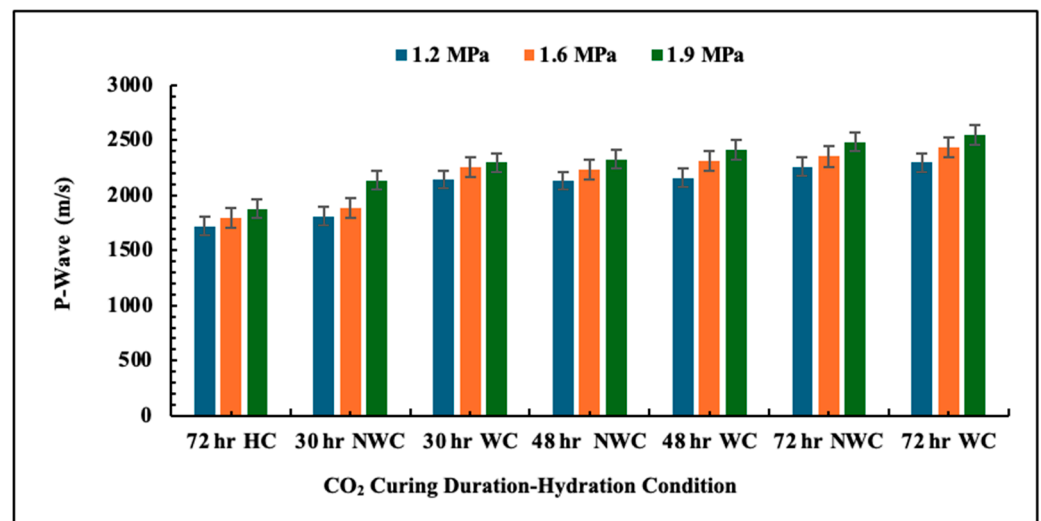

Figure 5. UNDT results for 0% TRC samples.

4.1.2. DT (Compression Test)

A minimum compressive strength of 3 MPa for non-structural bricks was the target strength in this study [54]. Figure 6 below shows the DT results of the samples tested with UNDT from Figure 5. Like the plots in Figure 5, the maximum strength was recorded for the WC samples compressed with 1.9 MPa, carbonated for 72 h, and soaked in water for another 72 h. Furthermore, 72 h carbonation was considered the optimum because, between 48 and 72 h carbonation, a marginal increase in strength was recorded. Hence, extending the carbonation duration beyond 72 h may not yield a remarkable increase in the strength and could lead to reduced strength which then translates to a waste of time and energy [69].

Table 2 below is a summary of the results obtained for the two testing methods, namely UNDT (P-wave) and DT (CS), the different compression pressures of 1.2, 1.6, and 1.9 MPa, and the three different curing approaches (HC, NWC, and WC) considered in this study.
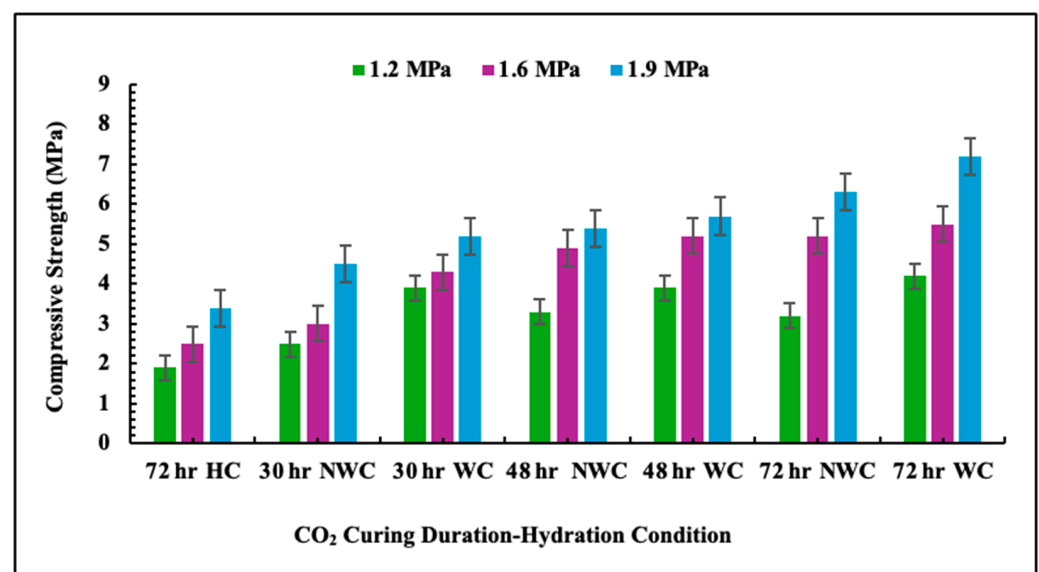
Figure 6. DT results for 0% TRC samples.

Table 2. Summary of UNDT and DT results considering varying compression pressures.

Compression Pressure (MPa)	P-Wave (m/s)	CS (MPa)	CO_2 Curing Duration—Hydration Condition
1.2	1721	1.9	72 h HC
	1813	2.5	30 h NWC
	2145	3.9	30 h WC
	2134	3.3	48 h NWC
	2159	3.9	48 h WC
	2260	3.2	72 h NWC
	2300	4.2	72 h WC
1.6	1800	2.5	72 h HC
	1885	3	30 h NWC
	2255	4.3	30 h WC
	2238	4.9	48 h NWC
	2311	5.2	48 h WC
	2354	5.2	72 h NWC
	2437	5.5	72 h WC
1.9	1880	3.4	72 h HC
	2138	4.5	30 h NWC
	2300	5.2	30 h WC
	2330	5.4	48 h NWC
	2414	5.7	48 h WC
	2486	6.3	72 h NWC
	2550	7.2	72 h WC

Additionally, UNDT and DT tests were performed on the samples produced with 5 and 10% TRC samples carbonated for 30, 48, and 72 h. Notably, a 1.9 MPa compression pressure was considered since it gave the maximum strength for the 0% TRC samples. After the carbonation durations, one set of samples (NWC) was tested, and the other set was subjected to post-carbonation curing (WC) for 72 h. From the UNDT results shown in Figure 7, the maximum velocities were associated with the samples subjected to post-carbonation curing (WC). Furthermore, in Figure 8, the 5% TRC samples carbonated for 72 h and water-cured (WC) had a maximum CS of 4 MPa. Though the strengths recorded for the 5% TRC samples were lower than the 0% TRC samples, the 5% TRC WC sample is reported to be suitable for non-load-bearing bricks for small buildings [54]. The lower strengths were due to reduced bonding and increased porosity within the rubberized matrix.
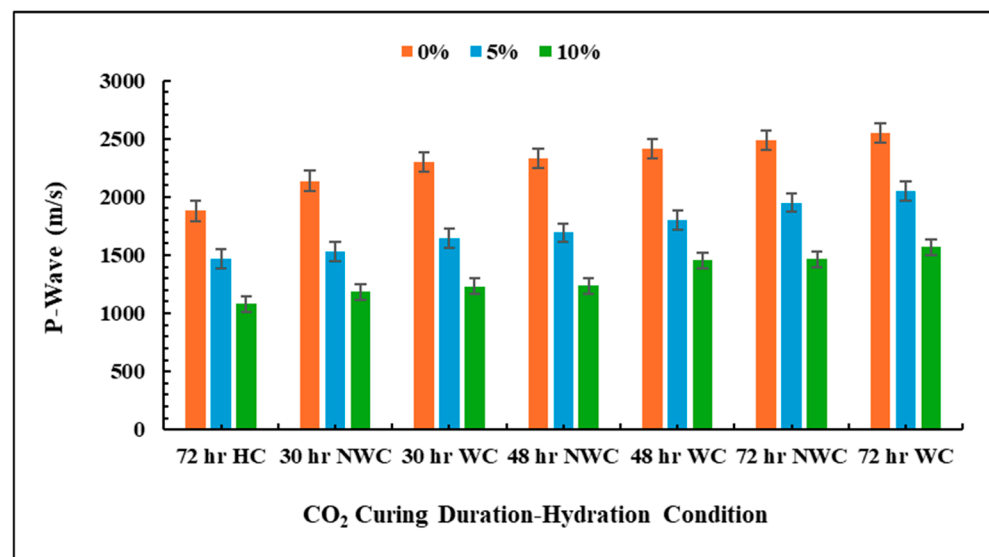
Figure 7. UNDT results considering 1.9 MPa compression pressure.
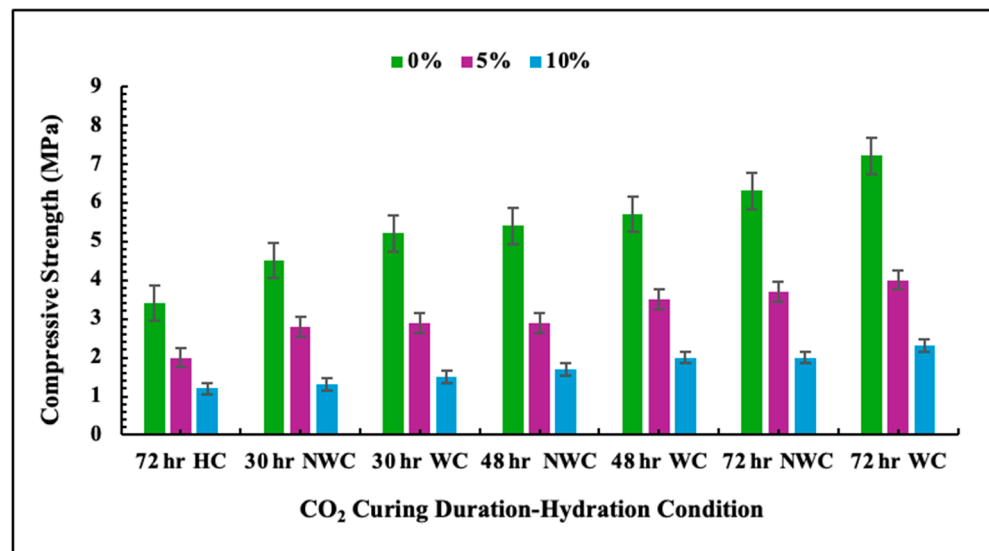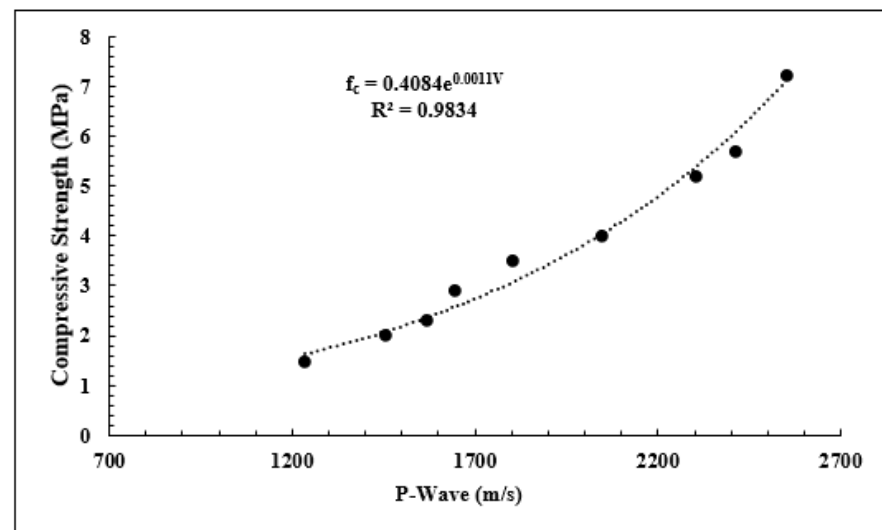

Figure 8. DT results considering 1.9 MPa compression pressure.

Table 3 is a summary of the results obtained for the two testing methods, namely UNDT (P-wave) and DT (CS), the varying TRC, and the three different curing approaches (HC, NWC, and WC) considered in this study.

From plots 7 and 8 above, it can be observed that a direct correlation exists between the UNDT and DT results. Since a direct correlation exists, models can be generated to establish this correlation. Research has also shown that different theoretical models have been developed to demonstrate the correlation between the wave velocities and CS in samples [26,37,70]. However, it is important to note that these correlations depend on factors such as the type of cementitious material, water cement/binder ratio, specimen size, curing duration, methods employed in testing the samples, and types of aggregate [39]. In this study, since the WC samples had the highest CS, linear, exponential, logarithmic, and power models were developed based on the results obtained for the WC samples. The exponential model with an acceptable trendline gave the most preferred relationship between the wave velocities and the CS for the 0, 5, and 10% TRC WC samples (Figure 9). A correlation coefficient (R^2) of 0.98 was obtained and was considered the most reliable coefficient.

Table 3. Summary of UNDT and DT results considering varying TRC.

TRC (%)	P-Wave (m/s)	CS (MPa)	CO$_2$ Curing Duration—Hydration Condition
0	1800	3.4	72 h HC
	2138	4.5	30 h NWC
	2300	5.2	30 h WC
	2330	5.4	48 h NWC
	2414	5.7	48 h WC
	2486	6.3	72 h NWC
	2550	7.2	72 h WC
5	1467	2	72 h HC
	1532	2.8	30 h NWC
	1646	2.9	30 h WC
	1694	2.9	48 h NWC
	1801	3.5	48 h WC
	1951	3.7	72 h NWC
	2050	4	72 h WC
10	1081	1.2	72 h HC
	1187	1.3	30 h NWC
	1234	1.5	30 h WC
	1239	1.7	48 h NWC
	1456	2	48 h WC
	1467	2	72 h NWC
	1571	2.3	72 h WC

Figure 9. An exponential relationship between the CS (f$_c$) and the P-wave velocities (V) for 0, 5, and 10% TRC WC samples.

The exponential model obtained in Equation (6) below can predict the laboratory compressive strength values for the 0, 5, and 10% TRC WC carbonated samples when cast samples are unavailable.

$$f_c = 4084e^{0.0011V} \tag{6}$$

where

f$_c$ = Compressive strength;
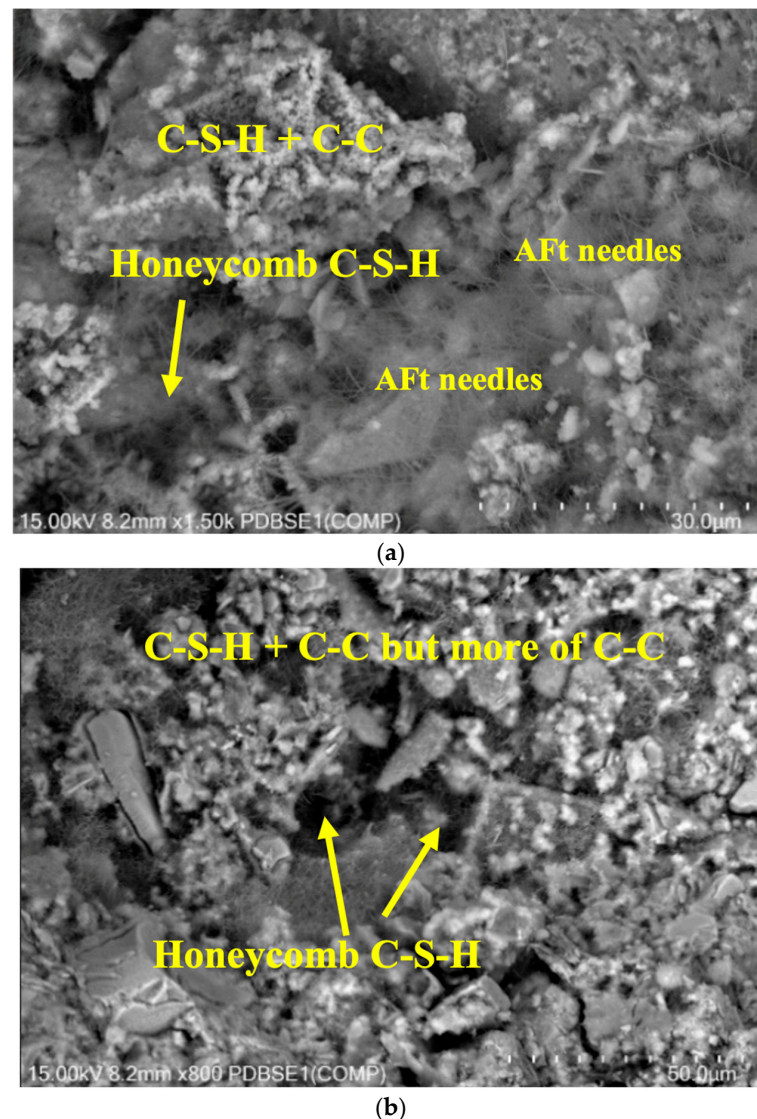V = Wave velocity.

The developed exponential model is a useful tool for predicting the CS of the carbonated samples produced in this study in an event where cast samples are unavailable. However, further investigation is recommended to verify the model considering different
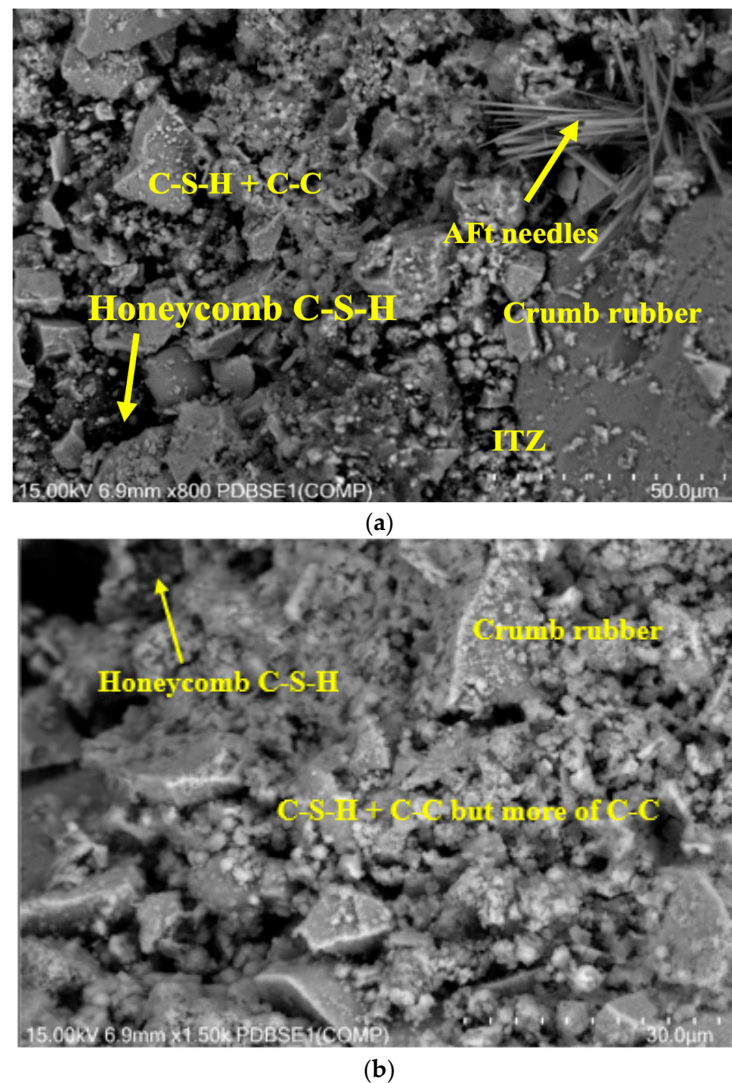
cementitious materials, water cement/binder ratios, specimen sizes, curing durations, methods employed in testing the samples, and types of aggregate from those used in this study.

4.2. Microanalysis (SEM and EDS)

The samples prepared with 0% and 5% TRC, compressed using 1.9 MPa, and carbonated for 72 h were analyzed using SEM, as shown in Figure 10a,b and Figure 11a,b, respectively. The WC samples prepared with 0 and 5% TRC were observed to have significant formations of calcium carbonate (C-C) and calcium silicate hydrates (C-S-H). This was due to the carbonation and post-carbonation hydration. For the samples that were not subjected to post-carbonation hydration, it was observed that there were more formations of C-C than C-S-H. This was mainly because the samples were only exposed to carbonation. Furthermore, the micrograph of the WC samples showed a conspicuous development of ettringite (AFt) needles in the form of needle-like crystals. These needles indicated that the post-carbonation hydration caused the samples to move into a crystalline phase, which was part of the hydration process required to replace the water lost during the preconditioning and the carbonation stages. The ettringite formation contributed to the additional strength recorded in the WC samples. For the NWC samples, AFt needles were not observed.

(a)

(b)

Figure 10. (**a**) SEM of 0% TRC sample (WC). (**b**) SEM of 0% TRC sample (NWC).

(**a**)

(**b**)

Figure 11. (**a**) SEM of 5% TRC sample (WC). (**b**) SEM of 5% TRC sample (NWC).

Additionally, honeycomb C-S-H was observed in both WC and NWC samples. Figure 12 shows enlarged images of the honeycomb formation. Shen et al. [71] reported that this type of C-S-H keeps a low density, owing to its elevated porosity. This is mainly because OPC was completely replaced LKD-GBFS, which disrupted the C-S-H from maturing.

The elemental analyses (EDS) of the samples (WC and NWC) are shown in Figure 13a,b and Figure 14a,b, respectively. The EDS revealed that the CC formed due to carbonation in the NWC samples was covered by honeycomb C-S-H, as evidenced by the high silicate (Si) content, in the carbonated samples. Furthermore, the WC samples had elevated the calcium (Ca) content due to the continuous hydration reactions when compared to the NWC samples. This was largely due to the different chemical processes that occurred during the carbonation and hydration processes. In addition, the post-carbonation hydration brought about an increased number of other elements that contributed to the higher strengths recorded for WC samples, as shown in Tables 4 and 5. Hence, the importance of post-carbonation hydration cannot be overemphasized and is recommended for samples exposed to ACC.
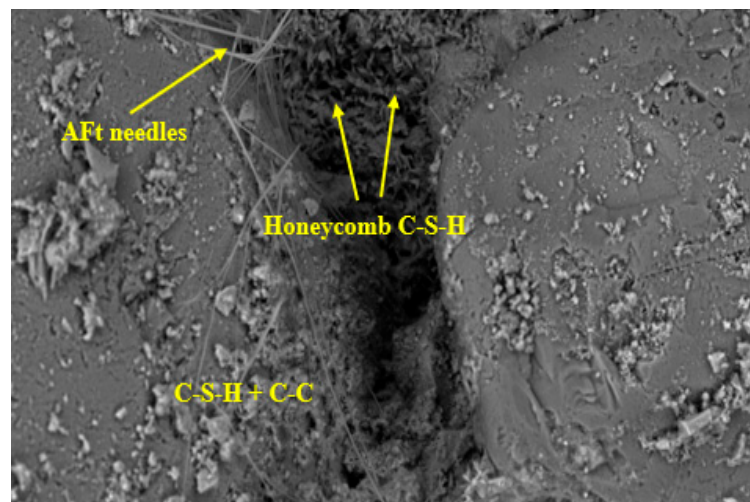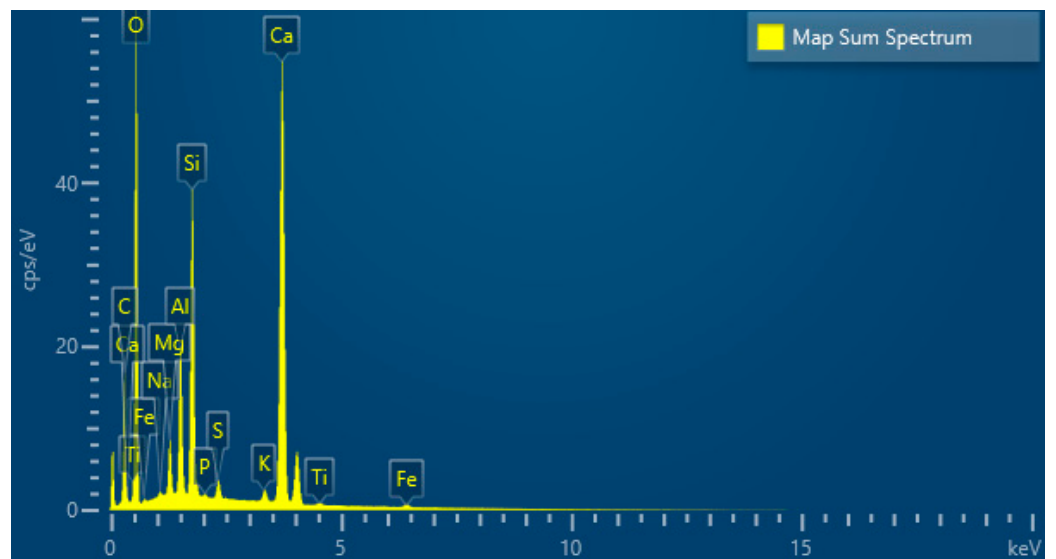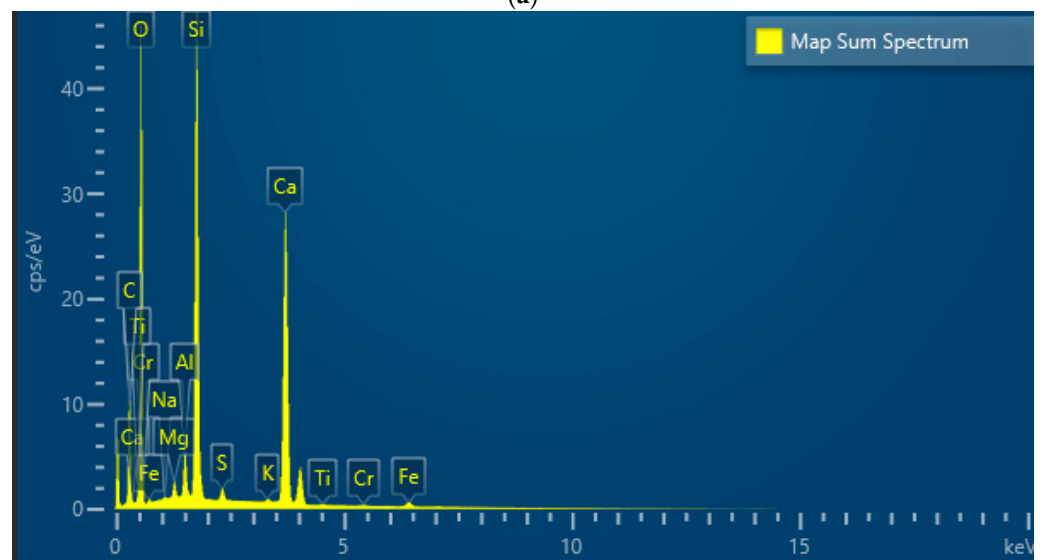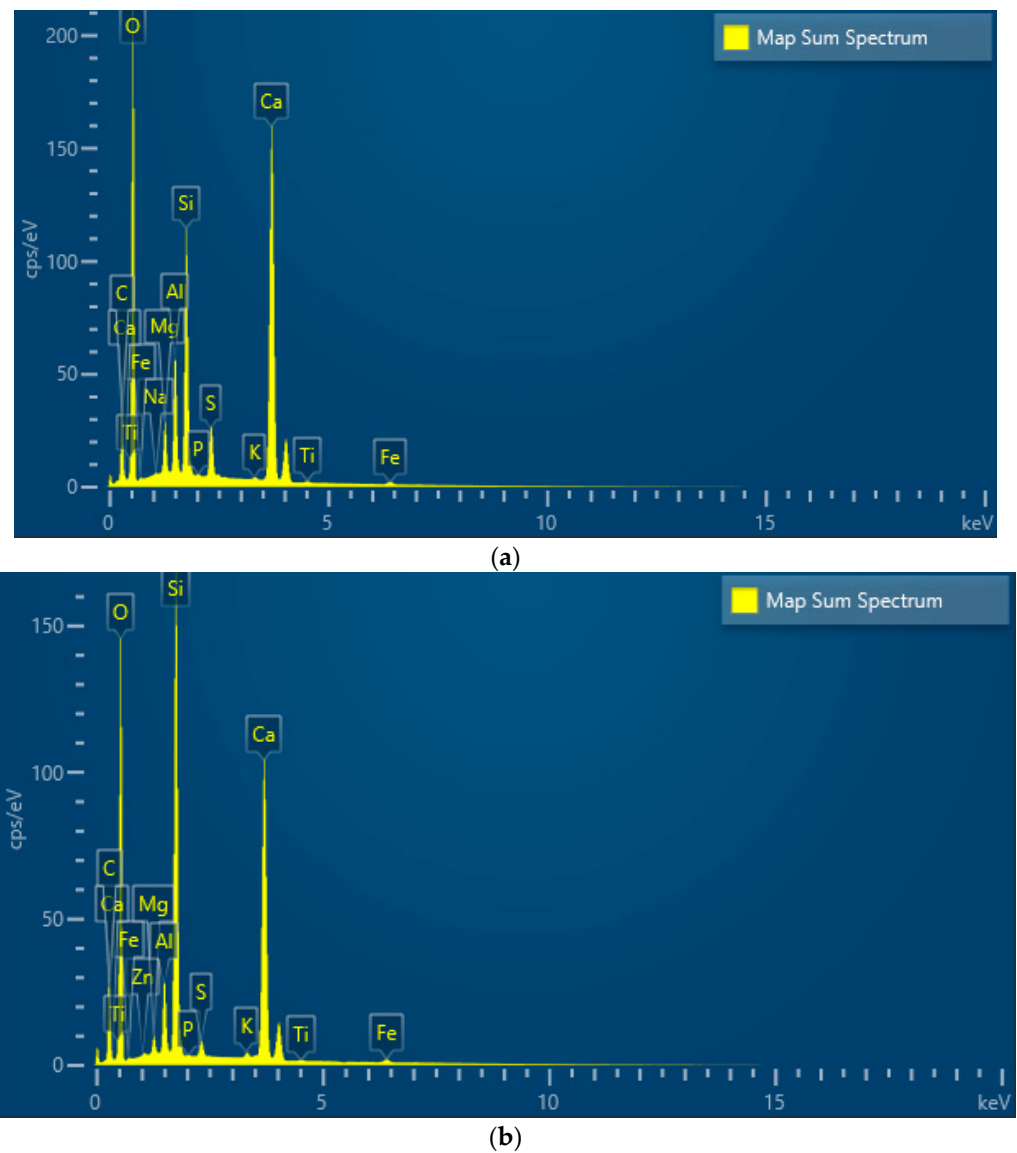
Figure 12. Honeycomb C-S-H (enlarged image).

(**a**)

(**b**)

Figure 13. (**a**) EDS of 0% TRC sample (WC). (**b**) EDS of 0% TRC sample (NWC).

(**a**)

(**b**)

Figure 14. (**a**) EDS of 5% sample (WC). (**b**) EDS of 5% sample (NWC).

Table 4. Elemental composition of 0% TRC (WC and NWC) samples.

	WC Samples		NWC Samples	
	Wt %	Wt % Sigma	Wt %	Wt % Sigma
C	13.83	0.16	19.66	0.17
O	45.17	0.14	50.45	0.13
Na	0.15	0.02	0.07	0.01
Mg	1.46	0.02	0.41	0.01
Al	3.78	0.03	1.00	0.01
Si	7.83	0.04	10.96	0.04
P	0.10	0.01	0.40	0.01
S	0.59	0.02	0.12	0.01
K	0.55	0.02	15.94	0.05
Ca	25.76	0.09	0.06	0.01
Ti	0.19	0.02	0.10	0.02
Fe	0.59	0.04	0.82	0.03
Total	100		100	

Table 5. Elemental composition of 5% TRC (WC and NWC) samples.

Map Sum Spectrum	WC Samples		NWC Samples	
	Wt %	Wt % Sigma	Wt %	Wt % Sigma
C	13.77	0.07	17.69	0.10
O	53.28	0.05	49.30	0.07
Na	0.06	0.01	0.49	0.01
Mg	1.41	0.01	1.79	0.01
Al	2.95	0.01	11.73	0.02
Si	5.99	0.01	0.04	0.00
P	0.05	0.00	0.53	0.01
S	1.71	0.01	0.23	0.01
K	0.12	0.00	17.39	0.03
Ca	20.00	0.03	0.09	0.01
Ti	0.13	0.01	0.65	0.01
Fe	0.53	0.01	0.08	0.01
Total	100		100	

4.3. CO_2 Uptake

The mass-gain method was used to calculate the CO_2 uptake within the samples. This method focuses on determining the CO_2 uptake of the entire sample as an average and providing an estimation of the CO_2 uptake by comparing the mass of the sample before and after carbonation. Equations (3) and (4) were used to compute the CO_2 uptake in all the samples.

Free water is necessary to facilitate the dissolution of CO_2; however, excess of it obstructs its penetration through the available porous path. Hence, pre-conditioning in a dry environment (RH = 55 ± 10%, T = 22 ± 3 °C) to create more capillary spaces for CO_2 sequestration into the samples for durations not exceeding 18 h is recommended by research [49,55].

Figure 15 shows the carbon uptake values for the 0% TRC samples considering the 1.2 and 1.6 MPa compression pressures applied to each layer. Overall, the samples compressed with 1.6 MPa had better carbon uptake when compared to samples compressed with 1.2 MPa. It can be assumed that the 1.2 MPa compression was insufficient to produce good contact within the particles in the matrix. Hence, the lower carbon uptake resulted in the low compressive strengths obtained. Figure 16 shows the carbon uptake of the 0, 5, and 10% TRC samples considering 1.9 MPa compression. From the results, the 1.9 MPa compression was sufficient for effective CO_2 sequestration, as recommended by Chang et al. [68]; hence, higher strengths were recorded.

Based on the information gathered from Figures 15 and 16, the total CO_2 uptake of the samples produced in this study was about 15,912 g (15.9 kg), which is in line with studies carried out by Hwalla et al. [33] and Xian et al. [65].

With the increasing awareness of achieving a net zero environment, a balance between the carbon dioxide emissions generated from construction activities and the amount removed through ACC is necessary. Hence, more research into ACC is encouraged, especially at the industrial level, to make the remarkable difference desired in climate change. Additionally, if brick-making factories can be set-up close to CO_2 emission sources, the CO_2 gas can easily be captured and utilized for curing. This will also allow costs to be saved for the long-distance transportation of the gas whereby leak risks are averted. Lastly, government and environmental agencies must establish incentives to motivate brick-making industries to accept and endorse the Advanced Carbon Technology (ACT). Incentives such as carbon capping, trading, and policies associated with taxation should be implemented to feature ACC as beneficial, thereby leading to a significant rise in annual CO_2 sequestration [12].
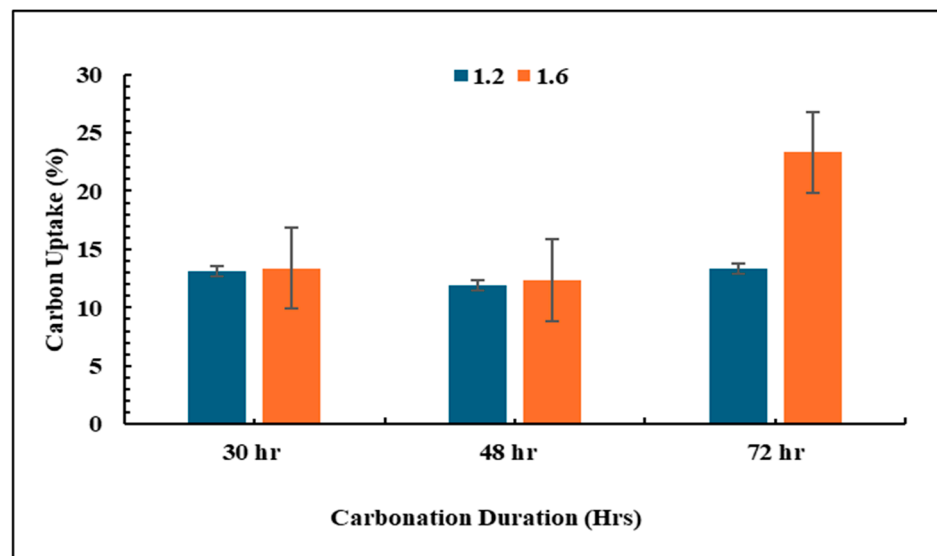
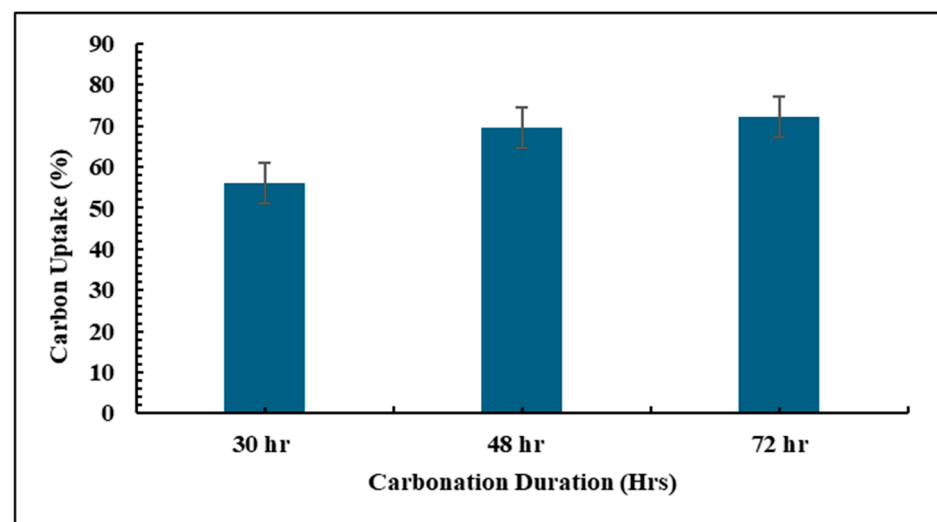**Figure 15.** CO_2 uptake for 0% TRC samples.

Figure 16. Effect of curing time on CO_2 uptake for samples compressed with 1.9 MPa pressure.

5. Conclusions

The CS of the samples produced in this study was examined using the UNDT and DT methods. From the experiments and analysis performed, the following conclusions can be made:

1. UNDT utilizing P waves is recommended as a quicker and reliable testing method, as seen in the study.
2. ACC is a recommended curing option that is environmentally friendly and saves curing time.
3. LKD-GBFS can be combined in a 60:40 (LKD:GBFS) blending ratio to produce load-bearing bricks with a CS of 7 MPa for building small houses [54]. This can be achieved by carbonating the samples for a 72 hr period and exposing the samples to post-carbonation hydration for another 72 h.
4. TRC can be replaced with up to 5% to produce non-load-bearing bricks which can be used for constructing small houses [54]. This can be achieved by carbonating the samples for a 72 hr period and exposing the samples to post-carbonation hydration for another 72 h.

5. The maximum CS values for the 0% TRC samples were 3, 6, and 7 MPa for the HC, NWC, and WC approaches, respectively. This indicated a 100% increment in CS between the HC and NWC samples. Similarly, for the 5% TRC samples, maximum CS values of 2, 3.7, and 4 MPa were recorded considering the respective curing approaches mentioned above. This again indicated an 85% increment in CS between the HC and NWC samples. The results have shown that for the same 72 h curing durations, the carbonated samples had double the strengths recorded for the HC samples. This highlights ACC as a quicker curing approach that guarantees improved strength in a green way.

6. Further hydration after carbonation is recommended to enhance the significant formations of calcium carbonate (C-C), calcium silicate hydrates (C-S-H), and ettringite needles, leading to improved strength after carbonation.

7. This utilization of LKD as sustainable waste in construction will contribute to addressing the problems associated with the disposal of LKD in landfills. Additionally, using waste tire crumbs as alternative aggregates to replace natural sand partially will aid in reducing the pressure exerted on the natural resources and prevent their gradual depletion.

8. The total CO_2 uptake of the samples produced in this study was about 15,912 g (15.9 kg). This figure shows that there is potential for ACT to bring about the desired climate change.

Author Contributions: J.A.O.: Formal Analysis. J.A.O. and H.A.-N.: Conceptualization, Methodology, Writing—original draft. H.A.-N.: Supervision, Validation: J.A.O., and H.A.-N.: Writing—review and editing. All authors have read and agreed to the published version of the manuscript.

Institutional Review Board Statement: Not applicable.

Informed Consent Statement: Not applicable.

Data Availability Statement: The data presented in this study are available on request from the corresponding author. The data are not publicly available due to ethical.

Conflicts of Interest: The authors hereby declare that they have no conflict of interest.

References

1. Wang, Y.; Zhu, Q.; Geng, Y. Trajectory and driving factors for GHG emissions in the Chinese cement industry. *J. Clean. Prod.* **2013**, *53*, 252–260. [CrossRef]

2. Gilfillan, D.; Marland, G.; Boden, T.; Andres, R. *Global, Regional, and National Fossil-Fuel CO₂ Emissions: 1751–2017, CDIAC-FF*; Research Institute for Environment, Energy, Economics, Appalachian State University: Boone, NC, USA, 2020. [CrossRef]

3. Summerbell, D.L.; Barlow, C.Y.; Cullen, J.M.J. Potential reduction of carbon emissions by performance improvement: A cement industry case study. *J. Clean. Prod* **2016**, *135*, 1327–1339. [CrossRef]

4. Farfan, J.; Fasihi, M.; Breyer, C. Trends in the global cement industry and opportunities for long-term sustainable CCU potential for Power-to-X. *J. Clean. Prod.* **2019**, *217*, 821–835. [CrossRef]

5. Cheng, D.; Reiner, D.M.; Yang, F.; Cui, C.; Meng, J.; Shan, Y.; Liu, Y.; Tao, S.; Dabo Guan, D. Projecting future carbon emissions from cement production in developing countries. *Nat. Commun.* **2023**, *14*, 8213. [CrossRef]

6. UNEP. *Global Status Report Towards a Zero-Emission, Efficient and Resilient Buildings and Construction Sector*; UNEP: Nairobi, Kenya, 2018.

7. World Bank. *Construction Industry Value Chain*; World Bank: Washington, DC, USA, 2018.

8. Gartner, E. Industrially interesting approaches to 'low CO_2' cements. *Cem. Concr. Res.* **2004**, *34*, 1489–1498. [CrossRef]

9. Hewlett, P.C. *Lea's Chemistry of Cement and Concrete*, 4th ed.; Hewlett, P.C., Ed.; Elsevier: Amsterdam, The Netherlands, 1998.

10. World Business Council for Sustainable Development: WBCSD. *The Cement Sustainability Initiative—Our Agenda for Action*; WBCSD: Geneva, Switzerland, 2002.

11. World Business Council for Sustainable Development: WBCSD. *Cement Technology Roadmap—Carbon Emissions Reductions up to 2050*; WBCSD: Geneva, Switzerland, 2009.

12. Oke, J.A.; Abuel-Naga, H.; Leong, E.C. De-carbonizing in Construction using Supplementary Cementitious Materials and Accelerated Carbonation Technique—A Review. *Int. J. Geotech. Eng.* **2024**, *18*, 1–22. [CrossRef]

13. Sizirici, B.; Fseha, Y.; Cho, C.-S.; Yildiz, I.; Byon, Y.-J. A Review of Carbon Footprint Reduction in Construction Industry, from Design to Operation. *Materials* **2021**, *14*, 6094. [CrossRef]

14. Intergovernmental Panel on Climate Change: IPCC. Sources of CO_2. In *IPCC Special Report on Carbon Dioxide Capture and Storage*; IPCC: Geneva, Switzerland, 2004; pp. 77–103.

15. Fernandez Pales, F.A.; Leung, Y. *Technology Roadmap-Low-Carbon Transition in the Cement Industry*; International Energy Agency: Paris, France, 2018.

16. International Energy Agency (IEA). *Energy Technology Perspectives 2017*; IEA: Paris, France, 2017.

17. United Nations Framework Convention on Climate Change—UNFCCC. In *Adoption of the Paris Agreement*; UNFCCCC: Bonn, Germany, 2015.

18. Rogelj, J.; Den Elzen, M.; Hohne, N.; Fransen, T.; Fekete, H.; Winkler, H.; Schaeffer, R.; Sha, F. Paris Agreement climate proposals need a boost to keep warming well below 2 °C. *Nature* **2020**, *534*, 1–10. [CrossRef]

19. National Oceanic and Atmospheric Administration: NOAA. *Climate at a Glance*; The Heartland Institute: Arlington Heights, IL, USA, 2020.

20. Intergovernmental Panel on Climate Change: IPCC. *Global Warming of 1.5 Degree*; IPCC: Geneva, Switzerland, 2019.

21. Jiang, K.; Ashworth, P.; Zhang, S.; Liang, X.; Sun, Y.; Angus, D. China's carbon capture, utilization and storage (CCUS) policy: A critical review. *Renew. Sustain. Energy Rev.* **2020**, *119*, 109601. [CrossRef]

22. Oke, J.A.; Olowoyo, M.K. Stabilization of laterite soil with eggshell powder and sodium silicate used as fill material in road construction. *Arid Zone J. Eng. Technol. Environ. AZOJETE* **2019**, *15*, 586–597.

23. Oke, J.A.; Obaji, N.O.; Osinubi, K.J. Oil palm empty fruit bunch ash stabilized laterite as a fill material for low-volume pavement. *Niger. J. Technol. NIJOTECH* **2020**, *39*, 721–731. [CrossRef]

24. Miah Md, J.; Huaping, R.; Paul, S.C.; Babafemi, A.J.; Li, Y. Long-term strength and durability performance of eco-friendly concrete with supplementary cementitious materials. *Innov. Infrastruct. Solut.* **2023**, *8*, 255. [CrossRef]

25. Aditto, F.S.; Sobuz, M.H.R.; Saha, A.; Jabin, J.A.; Kabbo, M.K.I.; Hasan, N.M.S.; Islam, S. Fresh, mechanical and microstructural behaviour of high-strength self-compacting concrete using supplementary cementitious materials. *Case Stud. Constr. Mater.* **2023**, *19*, e02395. [CrossRef]

26. Oke, J.A.; Abuel-Naga, H. Assessment of a Non-destructive Testing Method Using Ultrasonic Pulse Velocity to Determine the Compressive Strength of Rubberized Bricks Produced with Lime Kiln Dust Waste. *Geotechnics* **2023**, *3*, 1294–1308. [CrossRef]

27. Oke, J.A.; Abuel-Naga, H. Durability Assessment of Eco-Friendly Bricks Containing Lime Kiln Dust and Tire Rubber Waste Using Mercury Intrusion Porosimetry. *Appl. Sci.* **2024**, *14*, 5131. [CrossRef]

28. Zhu, C.; Fang, Y.; Wei, H. Carbonation-cementation of recycled hardened cement paste powder. *Constr. Build. Mater.* **2018**, *192*, 224–232. [CrossRef]

29. Chen, T.; Gao, X. Use of Carbonation Curing to Improve Mechanical Strength and Durability of Pervious Concrete. *ACS Sustain. Chem. Eng.* **2020**, *8*, 3872–3884. [CrossRef]

30. Bawab, J.; El-Hassan, H.; El-Dieb, A.; Jamal Khatib, J. Accelerated carbonation curing of concrete incorporating calcium carbide residue. *J. Build. Eng.* **2024**, *88*, 109258. [CrossRef]

31. Cardani, G.; Cantini, L.; Munda, S.; Zanzi, L.; Binda, L. Non invasive measurements of moisture in full-scale stone and brick masonry models after simulated flooding: Effectiveness of GPR. In *Nondestructive Testing of Materials and Structures*; Springer: Dordrecht, The Netherlands, 2013; pp. 1143–1149.

32. Aliabdo, A.A.E.; Elmoaty, A.E.M.A. Reliability of using nondestructive tests to estimate compressive strength of building stones and bricks. *Alex. Eng. J.* **2012**, *51*, 193–203. [CrossRef]

33. Hwalla, J.; Al-Mazrouei, M.; Al-Karbi, K.; Al-Hebsi, A.; Al-Ameri, M.; Al-Hadrami, F.; El-Hassan, H. Performance of Alkali-Activated Slag Concrete Masonry Blocks Subjected to Accelerated Carbonation Curing. *Sustainability* **2023**, *15*, 14291. [CrossRef]

34. Muthu, M.; Kumar, S.; Chajec, A.; Sadowski, Ł. Effect of EAF Slag on the Performance of Wollastonite Mixes Inspired by CO_2 Curing Technology. *Appl. Sci.* **2024**, *14*, 4485. [CrossRef]

35. Mohammed, B.S.; Azmi, N.J.; Abdullahi, M. Evaluation of rubbercrete based on ultrasonic pulse velocity and rebound hammer tests. *Constr. Build. Mater.* **2011**, *25*, 1388–1397. [CrossRef]

36. Lee, Y.H.; Oh, T. The Measurement of P-, S-, and R-Wave Velocities to Evaluate the Condition of Reinforced and Prestressed Concrete Slabs. Hindawi Publishing Corporation. *Adv. Mater. Sci. Eng.* **2016**, *2016*, 1548215. [CrossRef]

37. Choi, Y.; Kim, I.-H.; Lim, H.-J.; Cho, C.-G. Investigation of Strength Properties for Concrete Containing Fine-Rubber Particles Using UPV. *Materials* **2022**, *15*, 3452. [CrossRef]

38. Siddique, R.; Naik, T.R. Properties of concrete containing scrap-tire rubber—an overview. *Waste Manag.* **2004**, *24*, 563–569. [CrossRef]

39. Kawai, K.; Sugiyama, T.; Kobayashi, K.; Sano, S. Inventory Data and Case Studies for Environmental Performance Evaluation of Concrete Structures. *J. Adv. Concr. Technol.* **2005**, *3*, 435–456. [CrossRef]

40. Arulrajah, A.; Mohammadinia, A.; D'Amico, A.; Horpibulsuk, S. Effect of lime kiln dust as an alternative binder in the stabilisation of construction and demolition materials. *Constr. Build. Mater.* **2017**, *152*, 999–1007. [CrossRef]

41. Li, X.; Ling, T.-C.; Hung Mo, K. Functions and impacts of plastic/rubber wastes as eco-friendly aggregate in concrete—A review. *Constr. Build. Mater.* **2020**, *240*, 117869. [CrossRef]

42. Tempa, K.; Chettri, N.; Thapa, G.; Phurba Gyeltshen, C.; Norbu, D.; Gurung, D.; Wangchuk, U. An experimental study and sustainability assessment of plastic waste as a binding material for producing economical cement-less paver blocks. *Eng. Sci. Technol. Int. J.* **2022**, *26*, 101008. [CrossRef]

43. Figaredo, A.; Dhanya, M. Development of Sustainable Brick Materials Incorporating Agro-Wastes: An Overview. *Int. Res. J. Eng. Technol. (IRJET)* **2018**, *5*, 721–726.

44. Maraveas, C. Production of Sustainable Construction Materials Using Agro-Wastes. *Materials* **2020**, *13*, 262. [CrossRef]

45. Latif, M.; Naganathan, S.; Razak, H.; Mustapha, K. Performance of lime kiln dust as cementitious material. Procedia Engineering. In Proceedings of the 5th International Conference of Euro Asia Civil Engineering Forum (EACEF-5), Surabaya, Indonesia, 15–18 September 2015; Volume 125, pp. 780–787. [CrossRef]

46. Arube, G.E.; Akosubo, I.S.; Damini, R.G. Analysing the effects of steel fibres in concrete paving blocks. *Int. J. Civ. Eng. Constr. Estate Manag.* **2021**, *9*, 38–51.

47. Muhit, I.B.; Muhammad, T.; Raihan, M.T.; Nuruzzaman, M.D. Determination of mortar strength using stone dust as a partially replaced material for cement and sand. *Adv. Concr. Constr.* **2014**, *2*, 249–259. [CrossRef]

48. Kakrasul, J.; Parsons, R.; Han, P. *Lime Kiln Dust for Treated Subgrades*; The University of Kansas: Lawrence, KS, USA, 2017.

49. He, P.P.; Shi, C.J.; Tu, Z.J.; Poon, C.S.; Zhang, J.K. Effect of Further Water Curing on Compressive Strength and Microstructure of CO_2-cured Concrete. *Cem. Concr. Compos.* **2016**, *72*, 80–88. [CrossRef]

50. Tian, S.; Zhang, T.; Li, Y. Research on modifier and modified process for rubber-particle used in rubberized concrete for road. *Adv. Mater. Res.* **2011**, *243*, 4125–4130. [CrossRef]

51. Mohammadi, I.; Khabbaz, H.; Vessalas, K. Enhancing mechanical performance of rubberised concrete pavements with sodium hydroxide treatment. *Mater. Struct.* **2016**, *49*, 813–827. [CrossRef]

52. Guo, S.; Dai, Q.; Si, R.; Sun, X.; Lu, C. Evaluation of properties performance of rubber-modified concrete for recycling of waste scrap tire. *J. Cleaner Prod.* **2017**, *148*, 681–689. [CrossRef]

53. *AS 3700*; Masonry Structures. Standards Australia: Sydney, NSW, Australia, 2018.

54. *AS 4773.2*; Masonry in Small Buildings Construction. Standards Australia: Sydney, NSW, Australia, 2015.

55. El-Hassan, H.; Shao, Y.; Ghouleh, Z. Reaction Products in Carbonation-Cured Lightweight Concrete. *J. Mater. Civ. Eng.* **2013**, *25*, 799–809. [CrossRef]

56. Jang, J.G.; Kim, G.M.; Kim, H.J.; Lee, H.K. Review on recent advances in CO_2 utilization and sequestration technologies in cement-based materials. *Construct. Build. Mater.* **2016**, *127*, 762e773. [CrossRef]

57. Rostami, V.; Shao, Y.; Boyd, A.J. Durability of concrete pipes subjected to combined steam and carbonation curing. *Construct. Build Mater.* **2011**, *25*, 3345–3355. [CrossRef]

58. Shi, C.; He, F.; Wu, Y. Effect of pre-conditioning on CO_2 curing of lightweight concrete blocks mixtures. *Construct. Build Mater.* **2012**, *26*, 257–267. [CrossRef]

59. Baojian, Z.; Chisun, P.; Caijun, S. CO_2 curing for improving the properties of concrete blocks containing recycled aggregates. *Cem. Concr. Compos.* **2013**, *42*, 1–8. [CrossRef]

60. Shi, C.J.; Liu, M.; He, P.P.; Ou, Z.H. Factors Affecting Kinetics of CO_2 Curing of Concrete. *J. Sustain. Cement-Based Mater.* **2012**, *1*, 24–33. [CrossRef]

61. El-Hassan, H. Accelerated Carbonation Curing as a Means of Reducing Carbon Dioxide Emissions. *Cem. Ind. —Optim. Charact. Sustain. Appl.* **2020**, *32*, 1–26.

62. Berger, R.L.; Young, J.F.; Leung, K. Acceleration of hydration of calcium silicates by carbon-dioxide treatment. *Nat. Phys. Sci.* **1972**, *240*, 16–18. [CrossRef]

63. Young, J.F.; Berger, R.L.; Breese, J. Accelerated curing of compacted calcium silicate mortars on exposure to CO_2. *J. Am. Ceram. Soc.* **1974**, *57*, 394–397. [CrossRef]

64. El-Hassan, H.; Shao, Y. Early carbonation curing of concrete masonry units with Portland limestone cement. *Cem. Concr. Compos.* **2015**, *62*, 168–177. [CrossRef]

65. Xian, X.; Mahoutian, M.; Zhang, D.; Shao, Y.; Yu, Z. Carbon capture and utilization using cement-free concrete products via near-ambient pressure carbonation. *Int. J. Greenh. Gas Control.* **2024**, *134*, 104130. [CrossRef]

66. Mahoutian, M.; Shao, Y. Production of cement-free construction blocks from industry wastes. *J. Cleaner Prod.* **2016**, *137*, 1339e1346. [CrossRef]

67. *ASTM C1383-04*; Standard Test Method for Measuring the P-Wave Speed and the Thickness of Concrete Plates Using the Impact-Echo Method. ASTM: West Conshohocken, PL, USA, 2009.

68. Chang, J.; Li, Y.; Cao, M.L.; Fang, Y.F. Influence of Magnesium Hydroxide Content and Fineness on the Carbonation of Calcium Hydroxide. *Constr. Build. Mater.* **2014**, *55*, 82–88. [CrossRef]

69. Gilroy, B.; Black, L.; Thompson, D.; Hogan, R.; Holmes, N. *Effects of Accelerated Carbonation Curing on CO_2 Sequestration and on the Compressive Strength of Concrete Masonry Units*; CERI: Dublin, Ireland, 2020.

70. Demirboğa, R.; Türkmen, I.; Karakoç, M.B. Relationship between ultrasonic velocity and compressive strength for high-volume mineral-admixtured concrete. *Cem. Concr. Res.* **2004**, *34*, 2329–2336. [CrossRef]
71. Shen, W.; Zhang, W.; Wang, J.; Han, C.; Zhang, B.; Li, J.; Xu, G. The microstructure formation of C-S-H in the HPC paste from nano-scale feature. *J. Sustain. Cem. Mater.* **2019**, *8*, 199–213. [CrossRef]